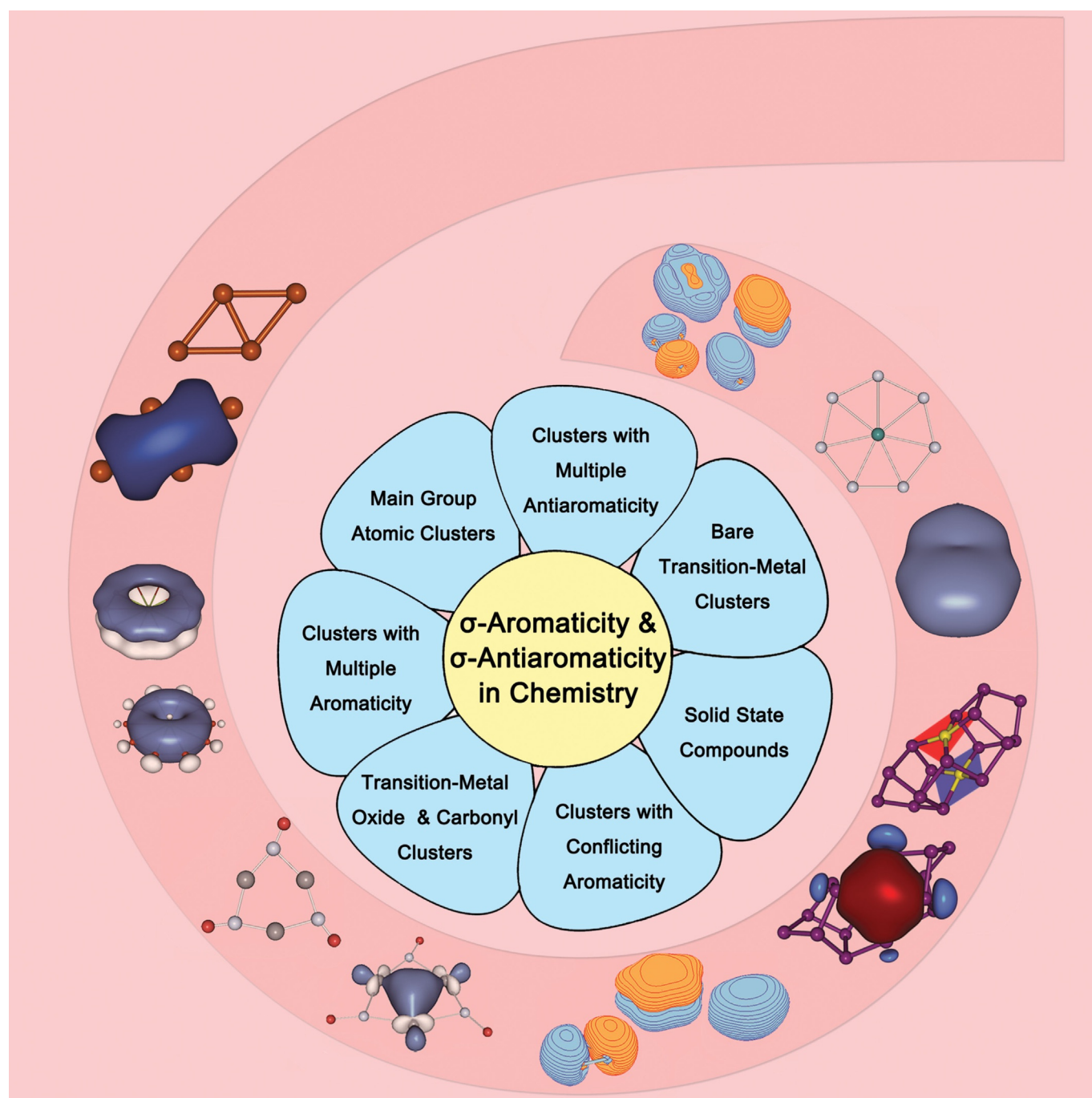


Chemical Bonding

# Usefulness of the $\sigma$ -Aromaticity and $\sigma$ -Antiaromaticity Concepts for Clusters and Solid-State Compounds

Ivan A. Popov,<sup>[a]</sup> Alyona A. Starikova,<sup>[b]</sup> Dmitry V. Steglenko,<sup>[b]</sup> and Alexander I. Boldyrev<sup>\*,[a, b]</sup>

*Dedicated to the memory of Professor Paul von Ragué Schleyer*



**Abstract:** In this Review we present examples of clusters, molecules, and solid-state compounds, for which the use of  $\sigma$ -aromaticity and  $\sigma$ -antiaromaticity concepts is essential for understanding of chemical bonding. We show that the bonding patterns in these  $\sigma$ -aromatic and  $\sigma$ -antiaromatic compounds are similar to those of the corresponding  $\pi$ -aromatic and  $\pi$ -antiaromatic chemical systems, respectively. Undoubtedly,  $\sigma$ -aromaticity helps us understand why the high symmetry isomers are the most stable among myriads of other potential structures. We also show that besides sys-

tems exhibiting either  $\sigma$ - or  $\pi$ -aromatic features, there are species, which can possess multiple aromaticity/antiaromaticity, or conflicting aromaticity patterns. We believe that the  $\sigma$ -aromaticity and  $\sigma$ -antiaromaticity concepts will be helpful in rationalizing chemical bonding, structure, stability, and molecular properties of chemical species in both organic and inorganic chemistry. We hope that they will also be useful for other areas of science such as material science, catalysis, nanotechnology, and biochemistry.

## $\sigma$ -Aromaticity and $\sigma$ -Antiaromaticity in Chemistry

Kekulé proposed the concept of aromaticity more than 150 years ago to explain the unusual low reactivity and high stability of benzene.<sup>[1–3]</sup> In 1931, Hückel introduced the electronic explanation of aromaticity by showing that cyclic molecules, which have  $4n + 2$   $\pi$  electrons should be considered aromatic, thus explaining their stability and reactivity features.<sup>[4,5]</sup>  $\pi$ -bonding in aromatic molecule is delocalized in nature and cannot be represented by a single Lewis structure. Later, using similar electronic considerations Breslow proposed a concept of antiaromaticity for molecules with  $4n$   $\pi$  electrons.<sup>[6,7]</sup> Contrary to aromatic species, antiaromatic molecules are expected to have low stability and high reactivity. These two concepts are widely accepted in chemistry and taught in various courses of chemistry including general chemistry classes. In addition to  $\pi$ -aromaticity, other aromaticity types were later proposed including  $\sigma$ -aromaticity,  $\delta$ -aromaticity, and even  $\phi$ -aromaticity. All these kinds of aromaticity are based on delocalized bonding of  $\sigma$ -,  $\pi$ -,  $\delta$ -, and  $\phi$ -electrons. The two last types of aromaticity are possible only if transition metals and f-elements are involved in delocalized bonding. Subsequently,  $\sigma$ -,  $\pi$ -,  $\delta$ -, and  $\phi$ -types of antiaromaticity were introduced. Furthermore, combination of different types of aromaticity/antiaromaticity was also shown to be feasible: multiple aromaticity, multiple antiaromaticity, and conflicting aromaticity (simultaneous presence of aromaticity and antiaromaticity of different types in a chemical species). These types of aromaticity are reviewed elsewhere.<sup>[8–21]</sup> Noteworthy, in spite of a significant number of papers published on these topics, these new aromaticity concepts still face skepticism and criticism.<sup>[22,23]</sup> Furthermore, we could not

find any mention of these types of aromaticity in the chemistry textbooks commonly used for education. Hence, the natural question is: are these aromaticity concepts useful or not?


Initially, the concept of  $\sigma$ -aromaticity was introduced in chemistry by Dewar,<sup>[24,25]</sup> who extended Hückel's aromaticity rule to the skeletal  $\sigma$ -type electrons to explain the anomalous magnetic behavior of cyclopropane. Afterwards, Schleyer and co-workers<sup>[26]</sup> showed that the  $\sigma$ -aromatic stabilization energy of cyclopropane relative to propane was only  $3.5 \text{ kcal mol}^{-1}$ , and therefore cyclopropane could not be considered a  $\sigma$ -aromatic molecule. In spite of this first failed case, the concept of  $\sigma$ -aromaticity continues to thrive in chemistry.

In this Review we would like to address the usefulness of  $\sigma$ -aromaticity and  $\sigma$ -antiaromaticity concepts in modern chemistry. In particular, here we show that these concepts are as important as the  $\pi$ -aromaticity and  $\pi$ -antiaromaticity concepts, which are well-accepted in organic chemistry. By means of a number of examples of various species, we demonstrate that the presence of the  $\sigma$ -delocalized bonding elements together with the thermodynamic stabilization/destabilization patterns define  $\sigma$ -aromaticity/antiaromaticity in any system. We also show that the features, which are commonly used to identify the  $\sigma$ -aromatic/antiaromatic compounds (stability, reactivity, electron delocalization), resemble those of prototypical  $\pi$ -aromatic/antiaromatic species, and, thus, should also be accepted and used by chemists in a similar manner.

In most of the studies presented here, chemical bonds were analyzed on the bases of completely delocalized canonical molecular orbitals (CMOs) and/or by utilizing electron localization schemes, that is, Natural Bond Orbital (NBO) analysis by Weinhold<sup>[27]</sup> and Adaptive Natural Density Partitioning (AdNDP) method written by Zubarev and Boldyrev.<sup>[28]</sup> In brief, AdNDP performs analysis of the first-order reduced density matrix with the purpose of obtaining its local block eigenfunctions with optimal convergence properties for describing the electron density. Similar to the NBO code, AdNDP allows determination of Lewis elements of localized bonding, such as one-center two-electron (1c–2e) bonds (lone pairs and core electrons), 2c–2e bonds (classical two-center two-electron bonds). Additionally, NBO can be used to search for 3c–2e bonds. In contrast to NBO, AdNDP enables delocalized bonds ( $nc$ –2e bonds,  $n > 3$ ) to be found if the remaining electrons cannot be localized into the 1c–2e, 2c–2e, and 3c–2e bonds. The user-directed form of

[a] Dr. I. A. Popov, Prof. Dr. A. I. Boldyrev  
Department of Chemistry and Biochemistry  
Utah State University  
Old Main Hill 300, Logan, Utah 84322 (USA)  
E-mail: a.i.boldyrev@usu.edu

[b] Dr. A. A. Starikova, Dr. D. V. Steglenko, Prof. Dr. A. I. Boldyrev  
Institute of Physical and Organic Chemistry  
Southern Federal University  
194/2 Stachka Ave., 344090 Rostov-on-Don (Russian Federation)

 The ORCID identification number(s) for the author(s) of this article can be found under <https://doi.org/10.1002/chem.201702035>.

the AdNDP analysis can also be applied to specified molecular fragments, and is analogous to the directed search option of the standard NBO code.

The delocalized (multicenter) bonds are usually associated with the concepts of aromaticity and antiaromaticity, though it should be pointed out that the presence of the delocalized bonding elements in a system is only necessary, but not a sufficient condition to claim aromaticity/antiaromaticity. As will be shown in the following sections, additional energy considerations should also be taken into account. In principle, the AdNDP procedure is numerically efficient because it involves only a series of diagonalizations of density matrix blocks. AdNDP accepts only those bonding elements whose occupation numbers (ONs) exceed the specified threshold values, which are usually chosen to be close to 2.00 |e|. Indeed, the AdNDP localization procedure is an approximation, and some electron density can be lost upon the transformation of the CMOs into the AdNDP bonds. Therefore, the ON values are given by non-integer numbers and are usually found in the range of 1.60–2.00 |e|. Still, we believe that the 80–100% electron density recovered for a bond is a very good qualitative approximation, which helps assess the presence, type, and strength of a bond on any fragment of the system of interest.

In most of the cases, the AdNDP results presented in this Review were obtained by using density functional theory (DFT) methods, though it was previously shown that the results of the AdNDP analysis do not generally depend on the choice of level of theory.<sup>[29]</sup> Recently, both NBO and AdNDP methods were extended to periodic systems,<sup>[30,31]</sup> thus allowing users to perform chemical bonding analyses in systems with periodic symmetry.

## $\sigma$ -Aromaticity and $\sigma$ -Antiaromaticity in Main Group Atomic Clusters

The primary application of  $\sigma$ -aromaticity in chemistry is with atomic clusters. In 2003 Alexandrova and Boldyrev proposed to use aromaticity to explain bonding in small alkali and alkaline-earth metal clusters.<sup>[32]</sup> They showed that the **Li<sub>3</sub><sup>+</sup> cluster was the smallest all-metal  $\sigma$ -aromatic cluster** with two delocalized  $\sigma$  electrons (Figure 1).

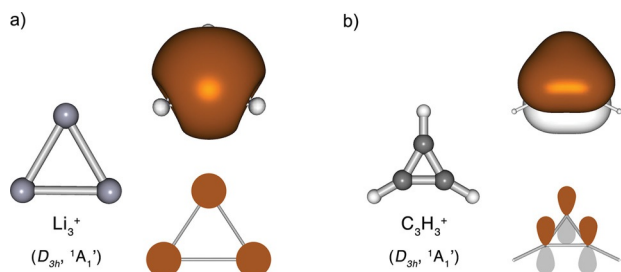


**Figure 1.** a) The structure of Li<sub>3</sub><sup>+</sup>, its HOMO (1a<sub>1</sub><sup>'</sup>), and a representation of the HOMO as a linear combination of 2s-AOs of the Li atoms. b) The structure of C<sub>3</sub>H<sub>3</sub><sup>+</sup>, its HOMO (1a<sub>2</sub><sup>'</sup>), and its representation as a linear combination of 2p<sub>z</sub>-AOs of C atoms.<sup>[32]</sup> Here and elsewhere the lines between atoms do not necessarily represent classical 2c–2e bonds. Reproduced from ref. [21].

One can see that the 1a<sub>1</sub><sup>'</sup> molecular orbital (MO) of Li<sub>3</sub><sup>+</sup> is a combination of the 2s atomic orbitals (AOs) of the three Li atoms (Figure 1 a), which is similar to the completely delocalized  $\pi$ -MO in C<sub>3</sub>H<sub>3</sub><sup>+</sup>, composed of 2p<sub>z</sub>-AOs of the C atoms (Figure 1 b). The C<sub>3</sub>H<sub>3</sub><sup>+</sup> molecule is commonly accepted as a  $\pi$ -aromatic species, since its two  $\pi$ -electrons are delocalized over the carbon triangle that satisfies the 4n + 2 rule (n = 0). Similar-

Ivan A. Popov obtained his B.S. (2009) and M.S. (2011) diplomas with honors in chemistry with an emphasis in physical chemistry from the Peoples' Friendship University of Russia, Moscow. Ivan received his Ph.D. from Utah State University under the direction of Professor Boldyrev. His research interests are focused on the computational design of novel materials for energy applications, analyses of their electronic structures, as well as development of chemical bonding models for novel clusters observed in experiments, and various periodically extended compounds.



Alyona A. Starikova received her diploma with honors in chemistry (2011) and her Ph.D. in physical chemistry from Southern Federal University (2013). She is currently a senior researcher at the Institute of Physical and Organic Chemistry at Southern Federal University. Her research interests include quantum organic and organometallic chemistry, and also the computational design of polyfunctional materials.



Dmitry V. Steglenko received his B.S./M.S. (2005) in chemistry from Rostov State University. In 2012 Dmitry obtained his Ph.D. in physical chemistry from Southern Federal University. His previous scientific work was related to the elucidation of mechanisms of cycloaddition reactions. His current research work is associated with the computational search for new two-dimensional systems and the study of their properties.



Alexander I. Boldyrev received his B.S./M.S. (1974) in chemistry from Novosibirsk University, his Ph.D. in physical chemistry from Moscow State University (1978), and his Dr. Sci. in chemical physics from Moscow Physico-Chemical Institute (1987). He is currently a Professor at the Department of Chemistry and Biochemistry at Utah State University. His current scientific interest is the development of new chemical bonding models for clusters, molecules, solid-state materials, novel two-dimensional materials, and other chemical species, where conventional chemical bonding models are not applicable.





ly, one should accept  $\sigma$ -aromaticity in  $\text{Li}_3^+$  due to the  $\sigma$ -delocalized MO. Indeed, both NBO and AdNDP analyses confirm the presence of the  $3c-2e$   $\sigma$ -bond in  $\text{Li}_3^+$ . Noteworthy, the  $\text{H}_3^+$  cation, being one of the most abundant ions in the universe and the smallest aromatic cluster, has the same two  $\sigma$ -electrons responsible for holding three atoms together, similar to the  $\text{Li}_3^+$  case.<sup>[33,34]</sup>

The importance of the  $\sigma$ -aromaticity concept may further be supported by the studies of the  $\text{Li}_2\text{Mg}_2$  cluster,<sup>[32]</sup> which show non-intuitive relative energy ordering of two different isomers (Figure 2).

Indeed, one could expect that a classical linear  $\text{Li-Mg-Mg-Li}$  structure with two  $2c-2e$   $\text{Mg-Li}$  and one  $2c-2e$   $\text{Mg-Mg}$   $\sigma$ -bonds would be the most stable structure for this cluster (Figure 2a). However, a diamond-shaped structure was found as a global minimum (Figure 2b), and was more stable than the linear isomer by approximately  $11 \text{ kcal mol}^{-1}$ . The reason for its stability was attributed to the formation of the  $\sigma$ -aromatic set composed of six delocalized electrons, which form three  $4c-2e$   $\sigma$ -bonds. This is an excellent example of how  $\sigma$ -aromaticity played a crucial role in determining the most stable cluster structure and helped explain why the cyclic isomer is more stable than the classical linear isomer.

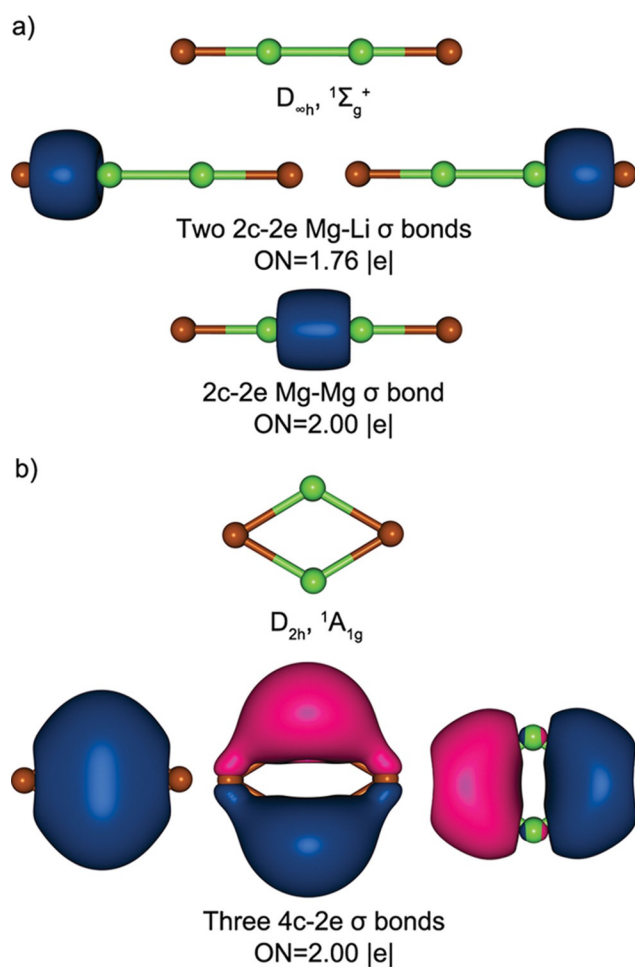


**Figure 2.** a) Linear isomer of the  $\text{Li}_2\text{Mg}_2$  cluster and its bonding pattern. b) Cyclic isomer and its bonding pattern. Color scheme: Mg: green, Li: brown. ON is equal to  $2.00 |e|$  in an ideal case.

The bare  $\text{Li}_4$  cluster has two electrons less than  $\text{Li}_2\text{Mg}_2$ , and thus is deemed to be antiaromatic ( $4n=4$ ,  $n=1$ ). The rhombus shape of the  $\text{Li}_4$  cluster is in accordance with the geometry of four-atomic  $\sigma$ -antiaromatic molecules with four  $\sigma$ -electrons. It was found that antiaromaticity originates from the  $\sigma$ -bonding  $\text{HOMO}-1$   $1a_g$  and  $\sigma$ -antibonding  $\text{HOMO}$   $1b_{1u}$  (Figure 3a). According to AdNDP, these two CMOs can be transformed into two localized chemical bonding objects, that is, two three-center bonds with  $\text{ON}=2.00 |e|$  (Figure 3b), which might also be viewed as two islands of local  $\sigma$ -aromaticity ( $4n+2=2$ ,  $n=0$  for each bond). Hence, the appearance of the  $\sigma$ -antiaromatic isomer as its global minimum for the  $\text{Li}_4$  cluster can be explained due to the local aromatic character of this cluster. Indeed, the use of the  $\sigma$ -aromaticity and  $\sigma$ -antiaromaticity concepts brings an important rationale of both geometric and electronic structures of such species.

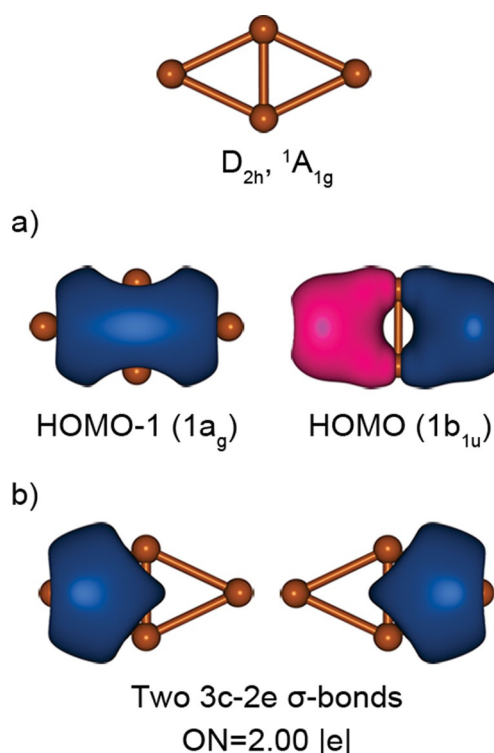


**Figure 3.** Global minimum structure of the  $\text{Li}_4$  cluster. a) Valence CMOs. b) Chemical bonding according to the AdNDP analysis.

### $\sigma$ -Aromaticity in Bare Transition-Metal Clusters

If only  $s$ -AOs are involved in chemical bonding, the cluster may either be  $\sigma$ -aromatic or  $\sigma$ -antiaromatic obeying the electron-counting rules  $4n+2/4n$  for a singlet coupling. Besides alkali and alkaline-earth metal atoms,  $\sigma$ -aromaticity/antiaromaticity can be found in transition metals. If we assume that only  $s$ -AOs participate in chemical bonding, while  $d$ -AOs are completely occupied in  $\text{Cu}$ ,  $\text{Ag}$ ,  $\text{Au}$ , one would expect that  $\text{Cu}_3^+$ ,  $\text{Ag}_3^+$ , and  $\text{Au}_3^+$  could be aromatic species as well, similar to  $\text{Li}_3^+$  and  $\text{H}_3^+$ . Indeed, Yong et al.<sup>[35]</sup> showed that all three cations have a perfect triangular structure, with a single com-

pletely bonding  $\sigma$ -MO. On the basis of the presence of the delocalized  $\sigma$ -MO, negative nuclear independent chemical shift (NICS)<sup>[36]</sup> values, and large resonance energy, they concluded that all these three cations are indeed  $\sigma$ -aromatic.

In 2003 Tanaka et al.<sup>[37]</sup> found that  $\text{Au}_5\text{Zn}^+$  was the most abundant cluster in the mass spectrum of  $\text{Au}_n\text{Zn}^+$  ( $n=2-44$ ). The authors performed quantum chemical calculations and identified the three lowest energy isomers I, II, and III for  $\text{Au}_5\text{Zn}^+$  (Figure 4).

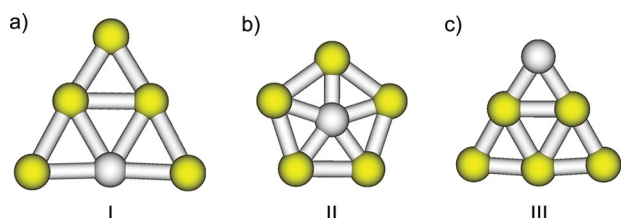


**Figure 4.** Optimized geometric isomers of the  $\text{Au}_5\text{Zn}^+$  cluster. Adapted with permission from ref.[37]. Copyright © 2003, American Chemical Society.

The MO patterns of isomers I and II depicted in Figure 5 resemble those of prototypical aromatic organic molecules  $\text{C}_6\text{H}_6$  and  $\text{C}_5\text{H}_5^-$ , except for their nodal properties in the molecular plane.

In both isomers, there are six delocalized electrons with the appropriate nodal patterns in  $\text{Au}_5\text{Zn}^+$  that satisfy the  $4n+2$

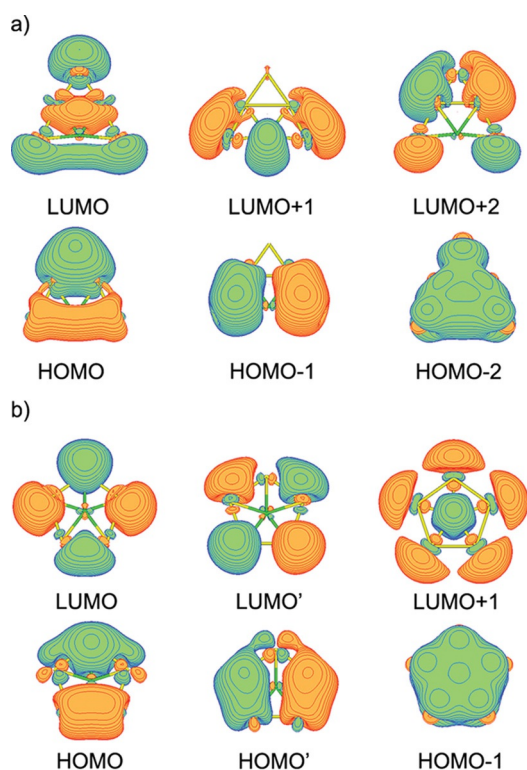


**Figure 5.** Pictures of valence CMOs of the  $\text{Au}_5\text{Zn}^+$  isomers I (a) and II (b). Adapted with permission from ref.[37]. Copyright © 2003, American Chemical Society.

rule for  $\sigma$ -aromaticity. Tanaka et al.<sup>[37]</sup> also performed NICS calculations for all three structures and concluded that the negative NICS values are comparable with those of  $\text{C}_6\text{H}_6$  and  $\text{C}_5\text{H}_5^-$ , thus confirming the presence of aromaticity in  $\text{Au}_5\text{Zn}^+$ . Hence, they concluded that the  $\text{Au}_5\text{Zn}^+$  cluster can be regarded as a  $\sigma$ -aromatic bimetallic cluster with six delocalized  $\sigma$ -electrons, and that the enhanced stability of  $\text{Au}_5\text{Zn}^+$  may be ascribed to its aromaticity. Interestingly,  $\text{Au}_5\text{Zn}^+$  is isoelectronic with the  $\text{Au}_6$  cluster, which was previously found to be an extremely stable electronic system with a record experimental HOMO–LUMO gap,<sup>[38,39]</sup> which hints at its  $\sigma$ -aromatic character as well.

Since then, many other  $\sigma$ -aromatic transition metal clusters have been reported, such as  $\text{Ag}_7^{3-}$ ,  $\text{Au}_7^{3-}$ ,  $\text{Au}_6\text{Y}^-$ ,  $\text{Cu}_7^{3-}$ ,  $\text{Cu}_7\text{Sc}$ ,  $\text{Cu}_7\text{Y}$ ,  $\text{Ag}_7\text{Y}$ , and  $\text{Au}_7\text{Y}$  (Figure 6).<sup>[40–43]</sup> The global minimum structures were found to have either ring or wheel-like geometries.

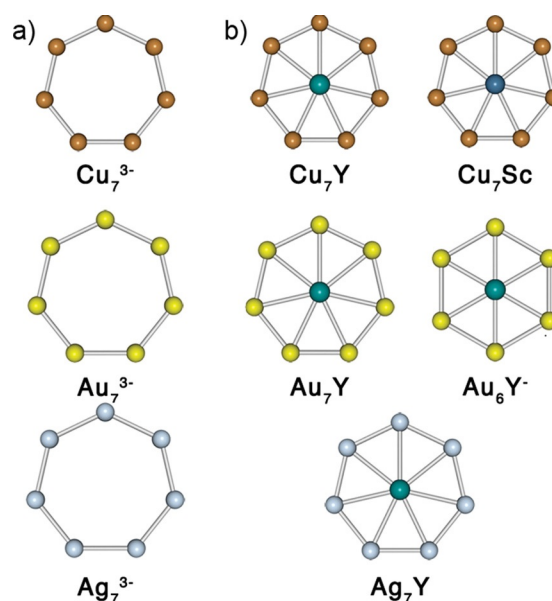


**Figure 6.** Geometric structures of a)  $\text{M}_7^{3-}$  ( $\text{M}=\text{Cu}, \text{Ag}, \text{Au}$ ). b)  $\text{Au}_6\text{Y}^-$  and  $\text{M}_7\text{L}$  ( $\text{M}=\text{Cu}, \text{Ag}, \text{Au}, \text{L}=\text{Sc}, \text{Y}$ ). Reproduced from ref.[16].

Lin et al.<sup>[43]</sup> showed that all these clusters are  $\sigma$ -aromatic species possessing 10 delocalized  $\sigma$ -electrons ( $4n+2=10$ ,  $n=2$ ). Let us consider the chemical bonding in one these clusters for example. The AdNDP analysis of the  $\text{Ag}_7\text{Y}$  cluster is shown in Figure 7.

The  $\text{Ag}_7\text{Y}$  cluster has 80 valence electrons if we include the 4d-AOs of Ag. One can see that the AdNDP method found five 4d-AO lone pairs (Figure 7a) on every Ag atom yielding 70 electrons. It also revealed five completely delocalized 8c-2e  $\sigma$ -bonds (Figure 7b) composed of 5s-AOs of Ag and 5s-AOs and 4d-AOs of Y yielding 10 electrons rendering this cluster  $\sigma$ -aromatic. The similar bonding picture was found for all these clusters. Indeed, the invoking of  $\sigma$ -aromaticity helps understand why they adopt such highly symmetrical structures, and why they are more energetically favorable than any other structures.

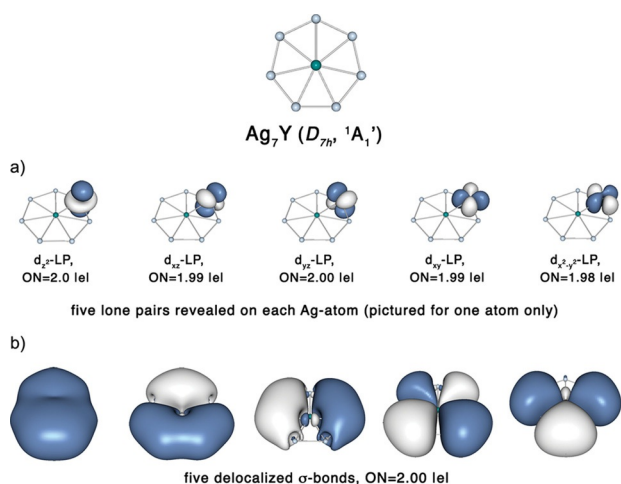


**Figure 7.** Geometric structure of Ag<sub>7</sub>Y. a) Five d-type lone pairs found on each Ag atom (shown on one atom only). b) Five delocalized 8c–2e  $\sigma$ -bonds. Reproduced from ref. [16].

## d-AO Based $\sigma$ -Aromaticity in Transition-Metal Oxide and Carbonyl Clusters

The  $M_3O_9^-$  (*D*<sub>3h</sub>, <sup>2</sup>A<sub>1</sub>) and  $M_3O_9^{2-}$  (*D*<sub>3h</sub>, <sup>1</sup>A<sub>1</sub>) (M=Mo and W) clusters were the first species where Huang et al. discovered d-AO based  $\sigma$ -aromaticity.<sup>[44]</sup> The electron counting of valence electrons in the  $M_3O_9^-$  and  $M_3O_9^{2-}$  clusters shows that if the oxidation states of oxygen are assumed to be –2, there are one and two extra electrons for the direct metal–metal bonding in  $M_3O_9^-$  and  $M_3O_9^{2-}$ , respectively. In all these high-symmetry anions two oxygen atoms are coordinated to each M atom, whereas the three other oxygen atoms form three M–O–M bridges. Analysis of the HOMOs in these species revealed that they are all completely bonding three-centered  $\sigma$ -bonds, thus rendering them  $\sigma$ -aromatic. Since the HOMOs are formed by the d-AOs of transition metal atoms, these species are examples of d-AOs based  $\sigma$ -aromatic molecular clusters.

Xu et al.<sup>[45]</sup> observed a remarkable planar  $Ti_3(CO)_3$  cluster under matrix isolation conditions.  $Ti_3(CO)_3$  consists of an equilateral triangular  $Ti_3$  core with side-on-bonded CO ligands (Figure 8).

Good agreement between calculated and experimental vibrational frequencies confirmed the structure. Based on the positive NICS values at the center of the Ti ring and 1 Å above (24.3 ppm and 14.8 ppm, respectively), the authors concluded that the cluster is antiaromatic. The assignment of the antiaromatic nature of this molecule was further questioned by Foroutan-Nejad et al.<sup>[46]</sup> They calculated NICS<sub>zz</sub> indices at three points (0.0, 0.5, and 1.0 Å) in and above the geometrical center of the  $Ti_3(CO)_3$  molecule. The corresponding values were found to be –117.9 ppm, –80.3 ppm, and –20.8 ppm, respectively, clearly indicating the presence of aromaticity. To resolve this controversy we performed the AdNDP analysis for the  $Ti_3(CO)_3$  molecule (Figure 8).<sup>[16]</sup> According to it, there are three  $\sigma$ -lone pairs (one on each oxygen, not shown in Figure 8), three triple ( $\sigma + 2\pi$ ) C≡O bonds, three 2c–2e C–Ti  $\sigma$ -bonds, three 3c–2e Ti–C–Ti  $\pi$ -bonds, one 3c–2e  $\sigma$ -bond delocalized over the  $Ti_3$  core,

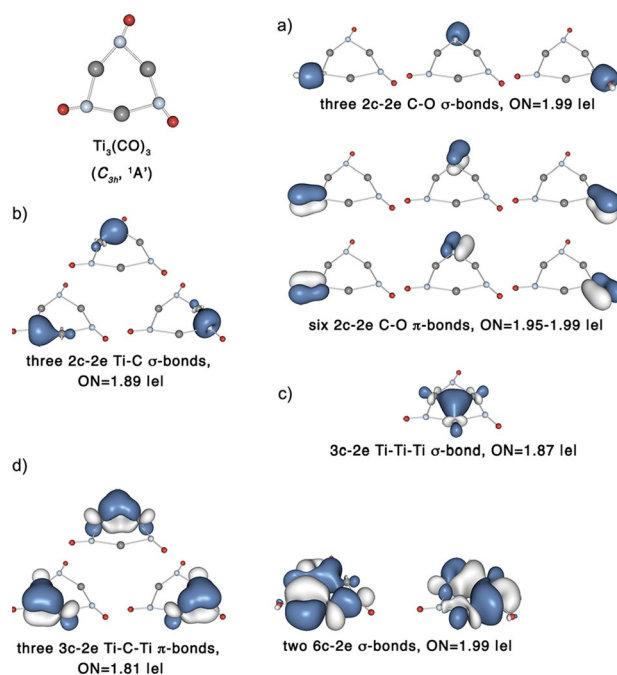


**Figure 8.** Geometric structure of  $Ti_3(CO)_3$ . a) Three 2c–2e C–O  $\sigma$ -bonds, six 2c–2e C–O  $\pi$  bonds. b) Three 2c–2e Ti–C  $\sigma$ -bonds. c) One 3c–2e Ti–Ti–Ti  $\sigma$ -bond. d) Two 6c–2e  $\sigma$ -bonds and three 3c–2e Ti–C–Ti  $\pi$ -bonds. Reproduced from ref. [16].

and two 6c–2e  $\sigma$ -bonds delocalized over the six-atom fragment consisting of three carbon and three titanium atoms. The six electrons occupying one 3c–2e and two 6c–2e bonds renders  $\sigma$ -aromaticity ( $4n + 2 = 6$ ,  $n = 1$ ) in this cluster, in accordance with the Foroutan-Nejad et al. conclusions.<sup>[46]</sup> Three 3c–2e Ti–C–Ti  $\pi$ -bonds make this cluster locally  $\pi$ -aromatic within each of the Ti–C–Ti triangles, but it was not considered as being a globally  $\pi$ -aromatic cluster. In the overall chemical bonding picture every CO ligand is coordinated to a Ti atom through a dative  $\sigma$ -bond and to two other Ti atoms through the 3c–2e Ti–C–Ti  $\pi$ -bonds (Figure 8). These 3c–2e bonds are formed of two electrons of each Ti atom with partial donation of these electrons to the antibonding  $\pi$ -bonds of CO ligands, so-called inverted donation. The occupation of the antibonding  $\pi$ -orbital in CO ligand is consistent with the significant weakening of the C≡O vibrational mode. According to Xu et al.<sup>[45]</sup> the <sup>12</sup>C<sup>16</sup>O stretch mode of the isolated CO molecule is 2143 cm<sup>–1</sup>, which weakens to 1398 cm<sup>–1</sup> in the  $Ti_3(CO)_3$  molecule. Hence, we have shown that the use of the  $\sigma$ -aromaticity is well justified to be used for understanding the structure and vibrational spectra of such interesting transitional-metal carbonyl molecule.

## $\sigma$ -Aromaticity in Solid-State Compounds

In recent years  $\sigma$ -aromaticity was extended into the solid state.<sup>[47–52]</sup> Robilotto et al.<sup>[47]</sup> reported the synthesis of the  $[(LAu)_3]^+ OTf^-$  compound with an  $Au_3^+$  core. The X-ray diffraction revealed that this compound is of approximate *D*<sub>3</sub> symme-



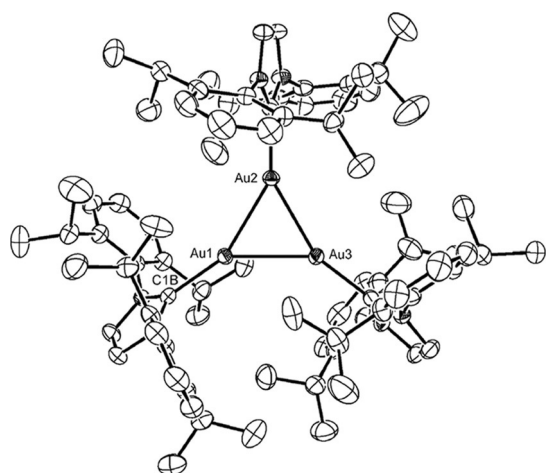


**Figure 9.** X-ray structure of the  $[(LAu)_3]^+$  ion. For clarity, H atoms, OTf anion and solvent are omitted. Reprinted with permission from ref.[47].

try, with the imidazolylidene rings canted by  $63.1(4)^\circ$  to  $77.7(4)^\circ$  (Figure 9).

The  $Au_3$  ring is nearly equilateral, with bond angles between  $59.603(9)^\circ$  and  $60.331(8)^\circ$ , and Au–Au distances from 2.6428(5) to 2.6633(5) Å. The DFT calculations of a model compound, in which *N*-methyl groups replaced the 2,6-diisopropenyl moieties, revealed a similar geometry with somewhat longer Au–Au distances of 2.705–2.706 Å. Chemical bonding analysis showed that the HOMO in this compound is similar to the HOMO in the  $Li_3^+$  cluster (see Figure 1). Based on this similarity, we believe that the  $Au_3^+$  core of this compound can also be considered as  $\sigma$ -aromatic.

Blanchard et al.<sup>[48]</sup> described the synthesis and characterization of the compound containing the triangular tripalladium cation  $[\{(SAr)(PAR)_3Pd\}_3]^+$  (Figure 10).

The crystals proved to be stable to oxygen and moisture at room temperature, and could be handled in air without any precaution. The three metal–metal distances in the complex are exactly equal at 2.8872(1) Å. The multinuclear NMR analysis

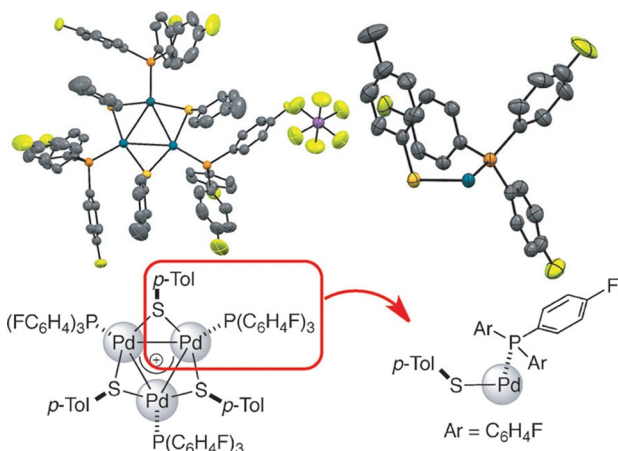


**Figure 10.** X-ray structure and asymmetric unit side view of the complex  $[\{(SC_6H_4)P(C_6H_4F)_3Pd\}_3]^+$ . Hydrogen atoms are omitted for clarity. Reprinted with permission from ref.[48].

of the complex indicated that the highly symmetric arrangement found in the solid state is maintained in solution. To gain more insight into the chemical bonding of this cluster, the authors performed DFT calculations of the model cluster,  $(PdSHPH_3)_3^+$ , in which the aromatic rings were replaced by hydrogen atoms. The follow-up AdNDP analysis revealed the presence of a 3c–2e bond between the three palladium atoms with a  $\sigma$ -like symmetry. The authors concluded that their compound contains the  $\sigma$ -aromatic noble-metal core.

Another example of a  $Pd_3$   $\sigma$ -aromatic compound  $[Pd_3Cl(PPh)_2(PPh_3)_3]^+[SbF_6]^-$  was reported very recently by Fu et al.<sup>[49]</sup> (Figure 11).

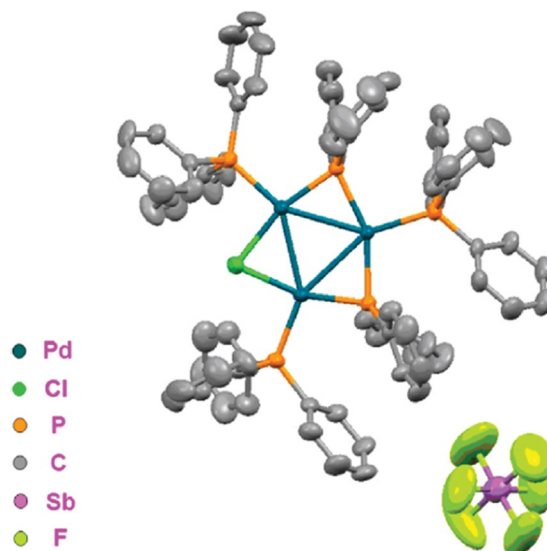


**Figure 11.** The crystal structure of  $[Pd_3Cl(PPh)_2(PPh_3)_3]^+[SbF_6]^-$ . Reprinted with permission from ref.[49]. Copyright © 2017, American Chemical Society.

According to the AdNDP analysis performed by the authors<sup>[49]</sup> for the simplified model cluster  $[Pd_3(PH_2)_3(PH_3)_3]^+$  (Figure 12a), there are twelve lone-pair 4d orbitals (*yz*, *zx*,  $x^2-y^2$ ,  $z^2$ ) on three Pd atoms with  $ON = 1.93\text{--}1.99$  |e| (Figure 12b),

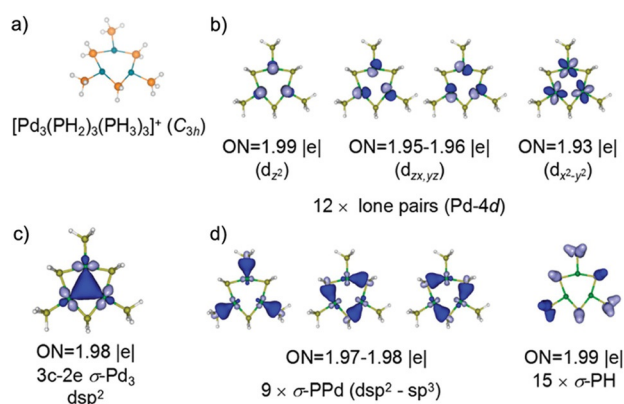


**Figure 12.** a) Optimized geometry of the  $[Pd_3(PH_2)_3(PH_3)_3]^+$  cluster. b), c) AdNDP chemical bonding. Adapted with permission from ref.[49]. Copyright © 2017, American Chemical Society.

one three-center delocalized Pd-Pd-Pd bond with  $ON=1.98 |e|$  (Figure 12c), fifteen P-H bonds with  $ON=1.99 |e|$ , and nine P-Pd bonds with  $ON=1.97-1.98 |e|$  (Figure 12d). The authors stated that the 3c-2e Pd-Pd-Pd bond was the reason for the Pd<sub>3</sub> stability. Again, the presence of the 3c-2e  $\sigma$ -bond is a sign of the  $\sigma$ -aromaticity.

Monfredini et al.<sup>[50]</sup> reported the synthesis and characterization of yet another compound containing the aromatic [Pd<sub>3</sub>]<sup>+</sup> core, which they called zwitterion **D** (Figure 13). They were able to decorate the all-metal aromatic [Pd<sub>3</sub>]<sup>+</sup> core with two different phosphinic ligands, a neutral and an anionic one. It was concluded that these clusters are definitely stable in the solid state, and proved to be remarkable precatalysts under transfer-hydrogenation conditions, highlighting the great potential of all-metal aromatics in catalysis.

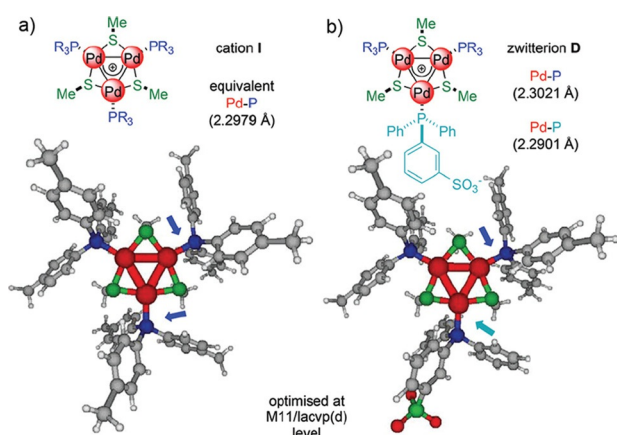


**Figure 13.** Comparison of optimized structures of cation **I** (a) and zwitterion **D** (b). The Pd-P distances in **D** at the M11/lacvp(d) level vary by +0.0041 and -0.0078 Å with the neutral and anionic phosphines, respectively. Adapted from ref. [50] with permission from the Royal Society of Chemistry.

Recently, Kuwabara et al.<sup>[51]</sup> prepared and characterized a compound containing the three-membered TiSn<sub>2</sub> ring core (Figure 14).

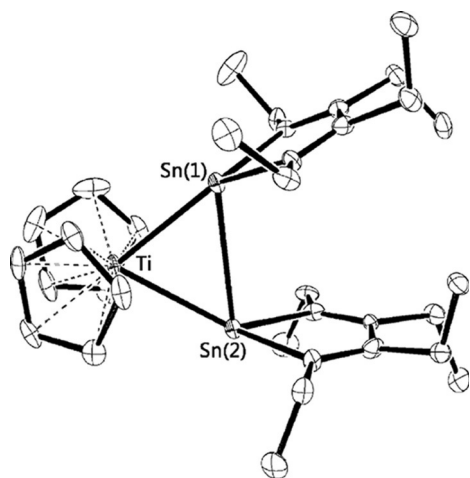


**Figure 14.** ORTEP representation of the Cp<sub>2</sub>Ti[SnC<sub>4</sub>Et<sub>4</sub>]<sub>2</sub> compound. All hydrogen atoms were omitted for clarity. Reprinted with permission from ref. [51].

The Ti-Sn bond lengths (2.6867(16) and 2.7254(17) Å) are appreciably shorter than the distances of previously reported T-Sn single bonds (2.842–2.984 Å). The distance between the two Sn atoms (3.0576(14) Å) is longer than the typical Sn=Sn bond length (2.575(4) to 2.85126(19) Å). All these geometric parameters hinted at the possibility of aromaticity in the TiSn<sub>2</sub> core. Indeed, complimentary chemical bonding analysis confirmed the presence of the  $\sigma$ -aromaticity in this core.

Importantly, in all the aromatic solid-state compounds discussed above we dealt with only one electron pair responsible for  $\sigma$ -aromaticity ( $4n+2=2$ ,  $n=0$ ). Last year the first solid-state compound containing two aromatic fragments with six  $\sigma$ -delocalized electrons each was reported by Popov et al.<sup>[52]</sup> The compound was isolated as a stable [K([2.2.2]crypt)]<sup>+</sup> salt and features a [Au<sub>2</sub>Sb<sub>16</sub>]<sup>4-</sup> cluster core possessing two all-metal aromatic AuSb<sub>4</sub> fragments (Figure 15).

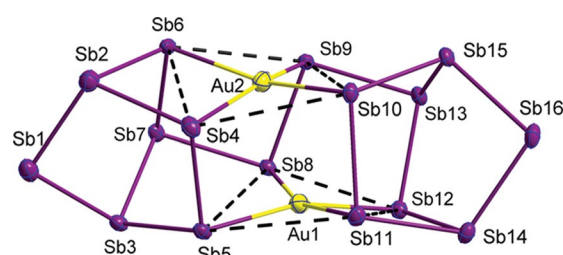


**Figure 15.** Thermal ellipsoid plot of the molecular cluster anion [Au<sub>2</sub>Sb<sub>16</sub>]<sup>4-</sup>. Reproduced from ref. [52].

The Au atoms are located at slightly distorted squares of four Sb atoms. In these quasi-planar AuSb<sub>4</sub> units, the Sb-Au-Sb bond angles are in the range of 82.35°–105.69° for Au1 and 82.67–107.96° for Au2. The Au-Sb bond lengths span a very narrow range  $2.69 \pm 0.02$  Å. The AdNDP analysis of the [Au<sub>2</sub>Sb<sub>16</sub>]<sup>4-</sup> cluster revealed 16 s-type lone pairs on 16 Sb atoms with  $ON=1.93-1.97 |e|$ , 2 p-type lone pairs on two peripheral Sb atoms (Sb1 and Sb16) with  $ON=1.71 |e|$ ; 19 classical 2c-2e Sb-Sb  $\sigma$ -bonds with  $ON=1.93-1.98 |e|$  responsible for the direct bonding between Sb atoms, 10 d-type electron pairs on two Au atoms (five on each) with  $ON=1.83-1.99 |e|$ . The remaining 12 electrons were found to participate in delocalized bonding: there are three 5c-2e  $\sigma$ -bonds with  $ON=1.86-1.99 |e|$  within each quasi-planar AuSb<sub>4</sub> fragment (Figure 16). These bonds look like classical  $\sigma$ -aromatic bonds: one is completely bonding and the other two have one nodal plane (mutually perpendicular), thus satisfying the  $4n+2$  rule for  $n=1$  in each fragment. Aromaticity in the AuSb<sub>4</sub> fragment was further confirmed by the electron-sharing indices ( $I_{ring}$  and MCI). This discovery is particularly important since the sextet of delocalized electrons was initially set at the heart of the aromaticity concept.



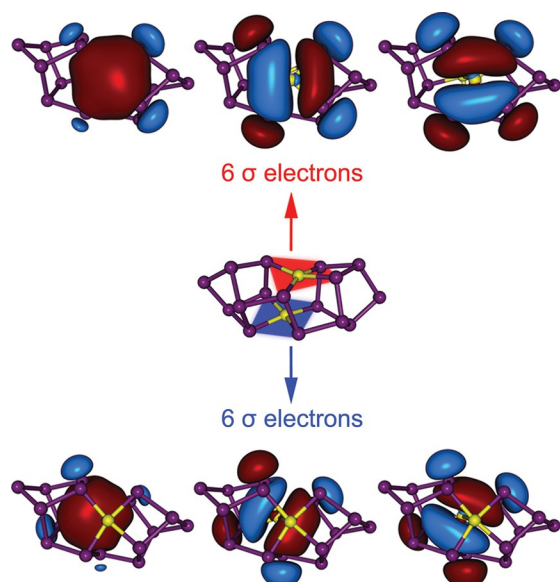


**Figure 16.** Delocalized chemical bonding elements deciphered for  $[\text{Au}_2\text{Sb}_{16}]^{4-}$ . Six  $5c-2e$  delocalized  $\sigma$  bonds with  $\text{ON} = 1.86-1.99 |e|$  found at upper  $\text{AuSb}_4$  ( $\text{Au}1-\text{Sb}5-\text{Sb}8-\text{Sb}11-\text{Sb}12$ ) and lower  $\text{AuSb}_4$  ( $\text{Au}2-\text{Sb}4-\text{Sb}6-\text{Sb}9-\text{Sb}10$ ) fragments. Reproduced from ref. [52].

### $\sigma$ -Aromaticity and $\sigma$ -Antiaromaticity in Clusters with Multiple Aromaticity, Conflicting Aromaticity, and Multiple Antiaromaticity

Introduction of  $\sigma$ -aromaticity and  $\sigma$ -antiaromaticity opens a possibility for double ( $\sigma$ - and  $\pi$ -) aromaticity, double ( $\sigma$ - and  $\pi$ -) antiaromaticity, and conflicting aromaticity (the simultaneous presence of either  $\sigma$ -aromaticity and  $\pi$ -antiaromaticity or  $\sigma$ -antiaromaticity and  $\pi$ -aromaticity). The double  $\sigma$ - and  $\pi$ -aromaticity was introduced in chemistry by Chandrasekhar et al. in 1979.<sup>[53]</sup> The extension of aromaticity and antiaromaticity into clusters showed a large diversity of combinations of such patterns.<sup>[8,10-21]</sup> In principle, one could imagine various combinations of aromaticity/antiaromaticity ( $\sigma$ -,  $\pi$ -,  $\delta$ -, and  $\phi$ -) including multifold aromaticity/antiaromaticity or conflicting aromaticity.<sup>[13]</sup>

A chemical species may be  $\sigma$ -aromatic or  $\sigma$ -antiaromatic if only  $s$ -AOs are involved in its delocalized bonding as we discussed before.  $\sigma$ -tangential ( $\sigma_t$ -),  $\sigma$ -radial ( $\sigma_r$ -), and  $\pi$ -aromaticity/antiaromaticity may possibly occur when only  $p$ -AOs are involved in delocalized bonding. In this case, the system can exhibit double ( $\sigma$ - and  $\pi$ -) aromaticity, double ( $\sigma$ - and  $\pi$ -) antiaromaticity, or conflicting aromaticity. If  $d$ -AOs are involved in delocalized chemical bonding, then  $\sigma_t$ -,  $\sigma_r$ -,  $\pi_t$ -,  $\pi_r$ -, and  $\delta$ -aromaticity/antiaromaticity can also occur. Therefore, the system can be multiply ( $\sigma$ -,  $\pi$ -, and  $\delta$ -) aromatic, multiply ( $\sigma$ -,  $\pi$ -, and  $\delta$ -) antiaromatic, or have conflicting aromaticity (simultaneous aromaticity and antiaromaticity of  $\sigma$ -,  $\pi$ -, or  $\delta$ -types). Finally, if  $f$ -AOs are involved in delocalized chemical bonding,  $\sigma_t$ -,  $\sigma_r$ -,  $\pi_t$ -,  $\pi_r$ -,  $\delta_t$ -,  $\delta_r$ -, and  $\phi$ -aromaticity/antiaromaticity patterns are expected. In this case, multiple ( $\sigma$ -,  $\pi$ -,  $\delta$ -, and  $\phi$ -) aromaticity, multiple ( $\sigma$ -,  $\pi$ -,  $\delta$ -,  $\phi$ -) antiaromaticity, and conflicting aromaticity are possible. Electron counting rules for aromaticity

and antiaromaticity for all these complicated cases have been reviewed elsewhere.<sup>[13]</sup> These tentative assignments of aromaticity are purely based on the presence of the appropriate delocalized bonding, but still other factors should be taken into account to claim that these assignments are correct. We will not discuss all these possible cases of aromaticity since that is beyond the scope of this Review. Instead, we will further focus on some specific cases, where  $\sigma$ -aromaticity and  $\sigma$ -antiaromaticity patterns were revealed in addition to other aromaticity types.

The first clusters where double ( $\sigma$ - and  $\pi$ -) aromaticity was found, were a series of binary  $\text{CuAl}_4^-$ ,  $\text{LiAl}_4^-$ , and  $\text{NaAl}_4^-$  species.<sup>[54,55]</sup> The search for the global minimum structures revealed that all these clusters have a pyramidal structure with the  $\text{Al}_4^{2-}$  square structure being a base and the  $\text{M}^+$  cation coordinated at top of the square. CMOs for the  $\text{Al}_4^{2-}$  cluster are shown in Figure 17.

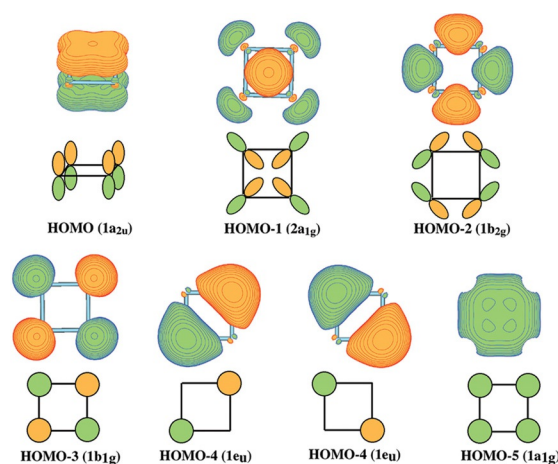


**Figure 17.** Valence CMOs of the  $\text{Al}_4^{2-}$  dianion. Adapted from ref. [54].

The HOMO ( $1a_{2u}$ ), HOMO-1 ( $2a_{1g}$ ), and HOMO-2 ( $1b_{2g}$ ) are completely bonding orbitals formed out of  $3p$ -AOs of Al and represent  $p_\pi$  ( $\pi$  orbitals perpendicular to the plane of the square from  $p_z$ -AOs),  $p_{\sigma-r}$  ( $\sigma$  orbitals are oriented radially towards the center of the square from the  $p_{x,y}$ -AOs), and  $p_{\sigma-t}$  ( $\sigma$  orbitals are oriented tangentially around the square from the  $p_{x,y}$ -AOs), respectively. The next four MOs are bonding, non-bonding, and antibonding orbitals formed primarily by the filled valence  $3s$  orbitals of Al. When all bonding, non-bonding, and antibonding MOs composed of the same AOs (such as the  $3s$  orbitals of Al in this case) are occupied, atomic lone pairs, which do not contribute much to chemical bonding, are formed. Thus, only three upper MOs are primarily responsible for the chemical bonding in  $\text{Al}_4^{2-}$ . If we split the  $\pi$ - (Figure 18a) and  $\sigma$ -orbitals (Figure 18b) into two separate sets, we can present the MOs formed by  $3p$ -AOs of Al by the MO diagram shown in Figure 18.

From this diagram one can see that  $\pi$ -electrons satisfy the  $4n+2$  rule for  $\pi$ -aromaticity. However, due to the simultaneous presence of the  $\sigma_r$  and  $\sigma_t$  counterparts, the  $4n+4$  rule is applied for  $\sigma$ -aromaticity in this case. The detailed discussion

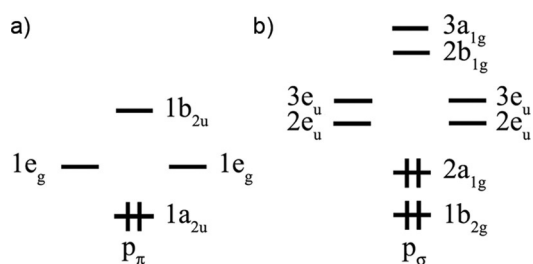


Figure 18. MO diagram of the  $\text{Al}_4^{2-}$  dianion.

about counting rules for all kinds of aromaticity/antiaromaticity cases is given elsewhere.<sup>[13]</sup> Overall, the totally delocalized  $\sigma$ -MOs ( $2a_{1g}$  and  $1b_{2g}$ ) make this cluster doubly  $\sigma$ -aromatic, while  $\pi$ -MO ( $1a_{2u}$ ) makes it  $\pi$ -aromatic. Noteworthy, the fact that all the global minimum structures of  $\text{MAl}_4^-$  ( $\text{M} = \text{Cu}, \text{Li}, \text{Na}$ ) clusters adopt similar pyramidal geometries with an  $\text{Al}_4^{2-}$  square base, and have relatively high experimental vertical electron detachment energies (VDE) 2.15 eV ( $\text{LiAl}_4^-$ ), 2.04 eV ( $\text{NaAl}_4^-$ ), and  $\text{CuAl}_4^-$  (2.32 eV) provides an additional proof for the aromaticity in these clusters.

We will briefly discuss two more cases of **double aromaticity** using the examples of  $\text{B}_9^-$  and  $\text{Ta@B}_{10}^-$  clusters, which were ex-

perimentally observed in a molecular beam.<sup>[56,57]</sup> Machine searches revealed that both clusters have very symmetrical wheel-like global minimum structures (Figures 19 and 20). Their structures were further confirmed by comparison of the experimental and theoretical VDEs.

The question is: why do these clusters adopt these beautiful symmetric structures? The **double aromaticity** helps answer this question. Let us first consider the  $\text{B}_9^-$  cluster. CMOs presented in Figure 19a can easily be interpreted for  $\pi$ -bonding. However, they are much more complicated for  $\sigma$ -bonding because it is not clear which orbitals contribute to the direct B–B bonds, and which orbitals are completely delocalized. To address that issue, we used AdNDP analysis that helped us obtain a much simpler chemical bonding picture. According to it, there are eight 2c–2e B–B  $\sigma$ -bonds on the periphery of the cluster, three 9c–2e delocalized  $\sigma$ -bonds, and three 9c–2e delocalized  $\pi$ -bonds.<sup>[56]</sup> The three delocalized  $\sigma$ -bonds make this cluster  $\sigma$ -aromatic, while the three delocalized  $\pi$ -bonds are responsible for the  $\pi$ -aromaticity. The presence of the double aromaticity perfectly explains the high symmetry of the global minimum structure of  $\text{B}_9^-$ , as well as its quite high first VDE of 3.46 eV (VDE of the  $\text{B}^-$  anion is only 0.277 eV).

The  $\text{Ta@B}_{10}^-$  cluster also has a wheel-type structure with a record high coordination number in the planar environment. The AdNDP analysis revealed that there are ten 2c–2e B–B  $\sigma$ -bonds constituting the periphery of the wheel, along with the delocalized bonding: five 11c–2e  $\sigma$ -bonds and three 11c–2e  $\pi$ -bonds (Figure 20). These multicenter bonds make this cluster doubly ( $\sigma$ - and  $\pi$ -) aromatic with  $n=2$  and  $n=1$ , respectively.

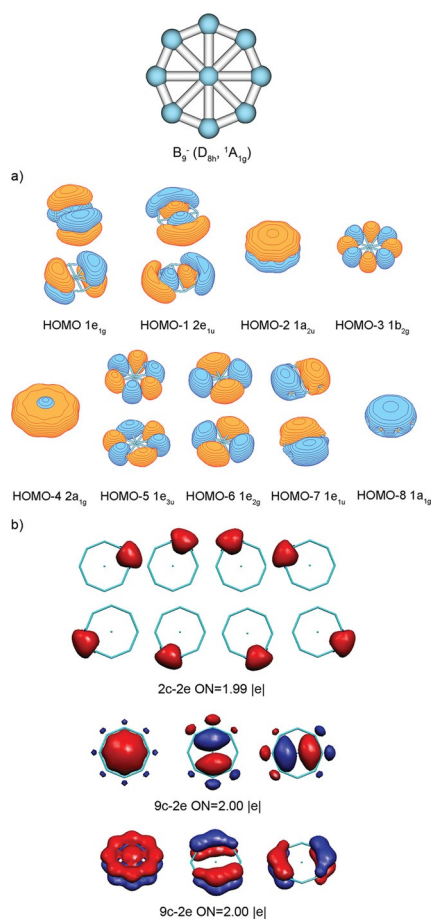


Figure 19. Structure of the  $\text{B}_9^- D_{8h}$  ( $^1A_{1g}$ ) cluster. a) CMOs. b) Results of the AdNDP localization. Adapted from ref. [28].

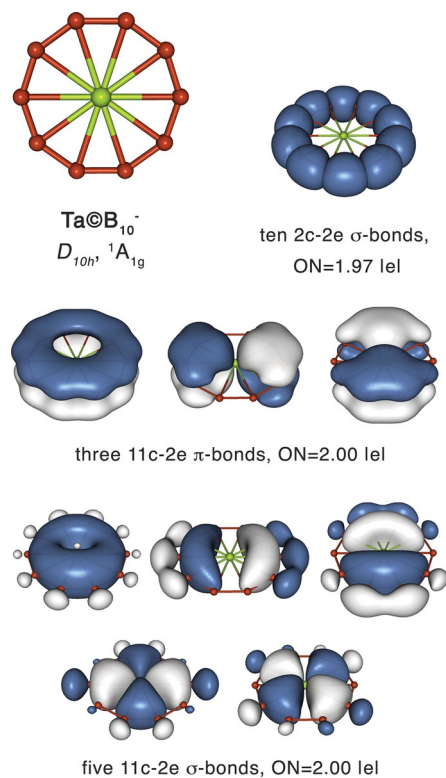


Figure 20. The structure of  $\text{Ta@B}_{10}^-$  and its chemical bonding pattern revealed by the AdNDP analysis. Adapted from ref. [57].

Again, a double aromaticity pattern helps us understand why this cluster adopts this high-symmetry planar structure as the global minimum with a high VDE of 4.04 eV.<sup>[57]</sup>

So far, we have discussed cases with double aromaticity. Let us now consider a case, where double ( $\sigma$ - and  $\pi$ -) antiaromaticity was found. The isolated  $B_6^{2-}$  cluster is an example of that.<sup>[58,59]</sup> The global minimum structure for the isolated  $B_6^{2-}$  cluster is a distorted hexagon of  $D_{2h}$  ( $^1A_g$ ) symmetry (Figure 21). It is easy to recognize the CMOs contributing to the delocalized  $\pi$ -bonding (Figure 21 a). Indeed, one may agree that the HOMO and HOMO-4 are responsible for the  $\pi$ -antiaromaticity. However, it is much more difficult to discern the number of localized and delocalized  $\sigma$ -bonding elements based only on the CMO picture. Thus, its structure seems very hard to understand. The AdNDP analysis simplifies this chemical bonding picture substantially (Figure 21 b). The analysis showed that the  $B_6^{2-}$  cluster has six classical peripheral 2c-2e B-B  $\sigma$ -bonds, two 3c-2e  $\sigma$ -bonds, and two 3c-2e  $\pi$ -bonds. As shown above on the example of the  $Li_4$  cluster, the overall delocalized bonds can be localized into sets of locally aromatic fragments in the case of the globally antiaromatic clusters. In principle,  $B_6^{2-}$  has two delocalized  $\sigma$ -bonds and two delocalized  $\pi$ -bonds, which can also be viewed as localized bonds: two 3c-2e  $\sigma$ -bonds and two 3c-2e  $\pi$ -bonds, respectively (Figure 21 b). We believe that even though this cluster is globally doubly antiaromatic, it is

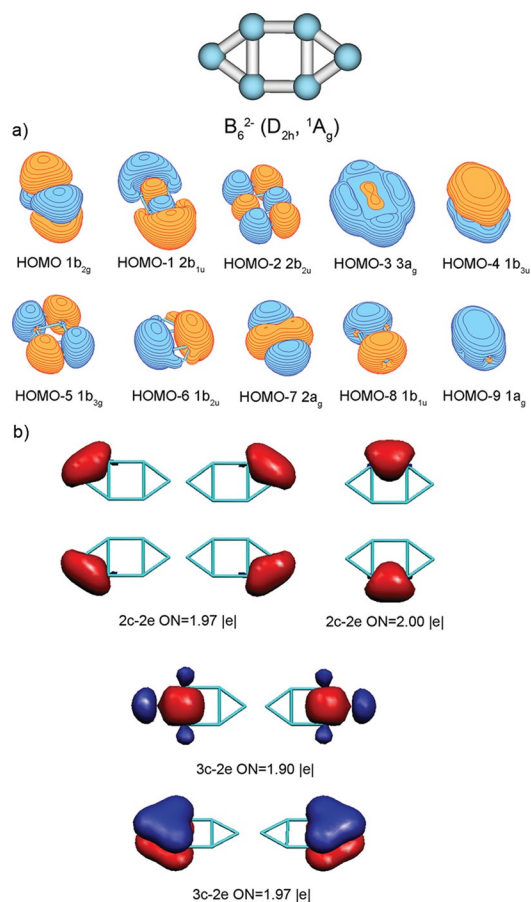


Figure 21. Structure of the  $B_6^{2-}$  cluster. a) CMOs. b) Results of the AdNDP analysis. Adapted from ref. [28].

locally doubly aromatic. That, in addition to the formation of the six 2c-2e  $\sigma$ -bonds, makes this structure more favorable over other alternative isomers.

It was previously shown that the doubly antiaromatic species were energetically competitive with aromatic ones in the example of the  $Si_4^{2-}$  cluster, which was experimentally observed in the form of the  $NaSi_4^-$  cluster.<sup>[60]</sup> Namely, Zhai et al. showed that the addition of two electrons to the neutral  $Si_4$  cluster leads to the formation of two energetically competitive isomers of  $Si_4^{2-}$ : a double antiaromatic ( $\sigma$ - and  $\pi$ -) parallelogram structure and an aromatic isomer with a butterfly distortion.

The  $B_5^-$  cluster is an interesting example in which the global minimum structure has conflicting aromaticity. It is a  $\sigma$ -antiaromatic and  $\pi$ -aromatic cluster (Figure 22).<sup>[11,61]</sup>

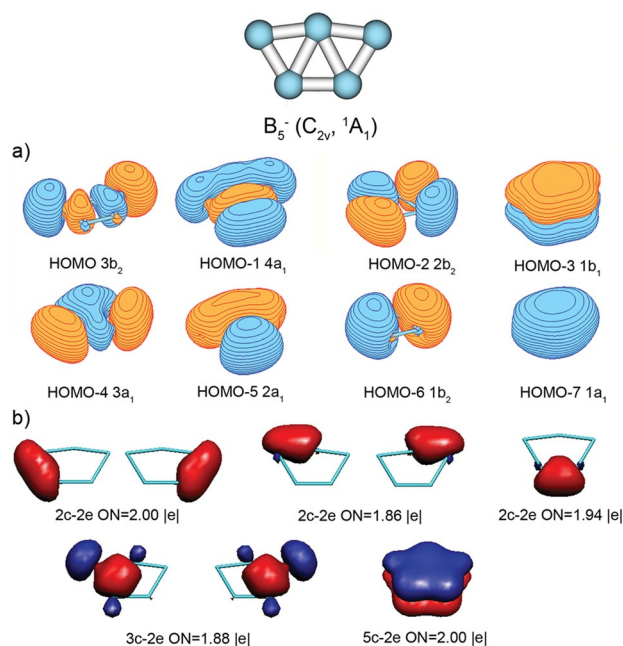


Figure 22. Structure of the  $B_5^-$  ( $C_{2v}$ ,  $^1A_1$ ) cluster. a) CMOs. b) Results of the AdNDP analysis. Adapted from ref. [28].

The CMOs of the most stable structure of the  $B_5^-$  cluster clearly show that this cluster is  $\pi$ -aromatic due to the presence of the HOMO-3 orbital (Figure 22 a). Therefore, it is unclear why this cluster does not adopt a perfect pentagon structure, as one would expect for the aromatic species. Again, the AdNDP analysis helped us address this question. We found that the distortion from the perfect pentagon comes from the  $\sigma$ -antiaromaticity factor. In addition to the five peripheral 2c-2e  $\sigma$ -bonds, AdNDP analysis revealed two delocalized  $\sigma$ -bonds responsible for its  $\sigma$ -antiaromatic character, which can also be found as two 3c-2e inner  $\sigma$ -bonds (Figure 22 b), similar to the  $B_6^{2-}$  cluster.

The  $Al_4^{4-}$  cluster, experimentally observed in the form of the  $Li_3Al_4^-$  cluster, represents a more famous example of a species exhibiting conflicting aromaticity.<sup>[62,63]</sup> Kuznetsov et al. showed that while two delocalized  $\sigma$ -bonding MOs (HOMO-1 and



HOMO–2) are responsible for the  $\sigma$ -aromaticity ( $\sigma_r$  and  $\sigma_r^-$ ) of the cluster, the HOMO and HOMO–4 make  $\text{Li}_3\text{Al}_4^-$   $\pi$ -antiaromatic.

The  $\text{Hf}_3$  cluster in its lowest singlet state (the ground state of this cluster is not yet established with certainty) is an example of triple ( $\sigma$ -,  $\pi$ -,  $\delta$ -) aromaticity.<sup>[64]</sup> The AdNDP analysis at the B3LYP/LANL2DZ level of theory is presented in Figure 23.

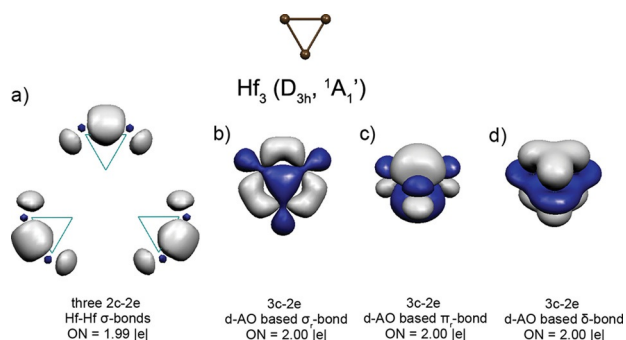


**Figure 23.** Geometric structure of  $\text{Hf}_3$ . a) Three 2c–2e Hf–Hf  $\sigma$ -bonds. b) 3c–2e d-AO based  $\sigma$ -bond. c) 3c–2e d-AO based  $\pi$ -bond. d) 3c–2e d-AO based  $\delta$ -bond. Adapted from ref. [16].

According to AdNDP,  $\text{Hf}_3$  has three 2c–2e Hf–Hf  $\sigma$ -bonds (Figure 23 a) formed by hybrid 6s-, 5d-AOs, and three completely delocalized bonds formed by pure d-AOs (one completely bonding 3c–2e d-AO based  $\sigma$ -bond (Figure 23 b), one completely bonding 3c–2e d-AO based  $\pi$ -bond (Figure 23 c), and one completely bonding 3c–2e d-AO based  $\delta$ -bond (Figure 23 d)). The 3c–2e d-AO based  $\delta$ -bond is formed by the overlap of the  $d_{z^2}$  atomic orbital on each Hf atom. One may rashly think of this peculiar bond as a  $\sigma$ - or  $\pi$ -bond. However, it is clear that this bond possesses two nodal surfaces, which is a characteristic of a  $\delta$ -bond. Thus, we have three delocalized bonds that are responsible for the presence of triple aromaticity.

Since this cluster is built of transition metal atoms, there is a question of the importance of the multiconfigurational character of the wave function. To check that, we performed AdNDP analysis at various levels of theory: **Hartree–Fock (HF), DFT (PBE0 method), coupled cluster (CCSD), and complete active space self-consistent field (CASSCF)** using a Stuttgart RSC 1977 ECP basis set and pseudopotential. The results of our calculations are presented in Table 1.

CASSCF(10,14) calculations showed an appreciable multiconfigurational character of the wave function (total of 2005003 configurations). The leading HF configuration has the coefficient

Bond <sup>[a]</sup>	HF	DFT	CCSD	CASSCF
2c–2e $\sigma$ -bonds	1.93	1.93	1.82	1.88
3c–2e $\pi$ -bond	2.00	2.00	1.91	1.87
3c–2e $\pi$ -bond	2.00	2.00	1.90	1.87

[a]  $R(\text{Hf–Hf}) = 2.73 \text{ \AA}$ .

of 0.838. Although the transition from HF and DFT to CCSD and CASSCF does lead to some changes in the ON values of the bonds, these changes are modest. Hence, we believe that these values firmly support our conclusion about the triple aromatic character of the  $\text{Hf}_3$  cluster.

The number of atomic clusters identified as doubly aromatic is growing rapidly,<sup>[8,10–21]</sup> but there is only one solid-state compound known, in which double  $\sigma$ - and  $\pi$ -aromaticity has been identified. That is the  $\text{Na}_3\text{Hg}_2$  amalgam.<sup>[65]</sup> The crystal structure of  $\text{Na}_3\text{Hg}_2$ <sup>[66,67]</sup> contains isolated  $\text{Hg}_4$  building blocks surrounded by sodium counter cations (Figure 24 a).

One can separate this crystal structure in the ionic limit into  $\text{Hg}_4^{6-}$  anions and  $\text{Na}^+$  cations. The double ( $\sigma$ - and  $\pi$ -) aromaticity of  $\text{Hg}_4^{6-}$  was recognized since it is valence isoelectronic to the doubly aromatic  $\text{Al}_4^{2-}$  cluster.<sup>[54]</sup> MO analysis of the isolated  $\text{Hg}_4^{6-}$  cluster revealed that neither 5d- nor 6s-AOs participate in chemical bonding (Figure 23 b). The 6p-AO-based MOs are responsible for bonding in this cluster. Three completely bonding orbitals formed by the  $\sigma_r$ -MO,  $\sigma_r^-$ -MO, and  $\pi$ -MO are responsible for the  $\sigma$ - and  $\pi$ -aromaticity in the cluster. However, chemical bonding analysis of a cluster with such high negative charge posts a question of its reliability. To address the influence of the other atoms of the crystalline lattice of the  $\text{Na}_3\text{Hg}_2$  amalgam, the AdNDP analysis was performed for the  $\text{Hg}_4^{6-}$  cluster embedded in the lattice (the cluster surrounded

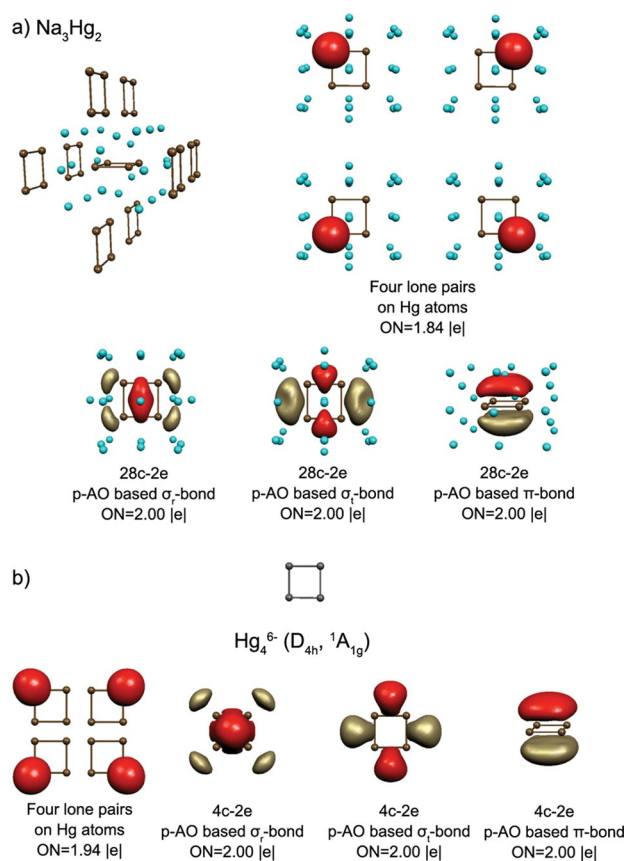


**Figure 24.** The bonding elements found by the AdNDP analysis for a)  $\text{Hg}_4^{6-}$  cluster embedded in a part of the crystalline lattice of  $\text{Na}_3\text{Hg}_2$  amalgam comprised out of 24 sodium cations placed at their position in the real crystalline structure and b) for the bare  $\text{Hg}_4^{6-}$  cluster. Adapted from ref. [15].

by 24 sodium cations located at the positions of the real  $\text{Na}_3\text{Hg}_2$  crystals).<sup>[15]</sup> The results show that the isolated and embedded clusters have essentially the same bonding pattern with some distortion imposed by the influence of sodium counterions. The delocalized bonds in the embedded cluster can no longer be presented as 4c–2e bonds. Instead, they are found as 28c–2e bonds, but the nodal structure of those 28c–2e bonds is exactly the same as in 4c–2e bonds of the bare  $\text{Hg}_4^{6-}$  cluster, thus confirming the overall pattern. This study clearly showed that the chemical bonding analysis of the bare multiply charged anion carrying a high additional charge could still be helpful in understanding chemical bonding of alloys. Overall, by using this example we showed that understanding the electronic structure of periodically extended systems by means of the aromaticity concepts greatly helps understand their geometrical parameters, and, thus, may further be used for the rational design of similar species with tailored properties.

## Conclusion and Outlook

All molecules and solid-state compounds discussed in this Review possess delocalized  $\sigma$ -bonding. As a matter of fact, chemical bonding in those species cannot be represented by a single Lewis structure. In all of them, lines between atoms do not necessarily represent traditional 2c–2e bonds, but a short distance between atoms. In case there are not enough electrons to make such 2c–2e bonds, concepts of delocalized ( $\sigma$ -,  $\pi$ -,  $\delta$ -, and  $\phi$ -) bonding are crucial. Indeed, it is hard to propose a single Lewis structure for clusters like  $\text{Au}_5\text{Zn}^+$  or  $\text{Ta@B}_{10}^-$ , which can be used in the follow-up valence bond calculations. On the other hand,  $\sigma$ -aromaticity allows us to explain why these species adopt such high-symmetry structures, and why  $\sigma$ -antiaromatic species are not that symmetric. Indeed, one can argue that the presence of delocalized bonding is not enough to claim aromaticity. Hence, it is necessary to find substantial resonance energy in these clusters or show their high stability or low reactivity in order to call such clusters aromatic. Well, even for the prototypical aromatic molecule benzene there is still no consensus on the value of the resonance energy.<sup>[68–70]</sup> Thus, we believe it is hopeless to try to find resonance energies, which will satisfy everybody.

Furthermore, it is widely accepted in organic chemistry that judgment on aromaticity can be based on the electronic factor, for example, the  $4n+2$  rule for  $\pi$ -aromaticity. Similar rules have been derived for  $\sigma$ -aromatic molecules.<sup>[13]</sup> However, we know that the  $4n+2$  rule does not always work even for  $\pi$ -aromaticity. Probably, the most famous case is the  $\text{N}_6$  molecule, which is isoelectronic to benzene. While the planar hexagonal structure of benzene is by far (about  $60 \text{ kcal mol}^{-1}$ ) the most stable structure among all possible isomers of the  $\text{C}_6\text{H}_6$  stoichiometry,<sup>[71]</sup> the perfect hexagon of  $\text{N}_6$  is not even a local minimum on the potential energy surface.<sup>[72,73]</sup>

While we believe that the counting rules (like  $4n+2$ ) for  $\sigma$ -aromaticity can be used as the starting point to claim aromaticity, some energy considerations should also be taken into account. From our point of view, the simplest way to assess

the contribution of aromaticity to bonding is to see if the species of interest is actually the most stable one among alternative isomers. It certainly works for benzene, where its planar hexagon isomer is the global minimum. If we accept this criterion, we can assign  $\sigma$ -aromaticity for all global minimum structures exhibiting delocalized  $\sigma$ -bonding. Indeed, the  $\sigma$ -aromaticity of the  $\text{Au}_5\text{Zn}^+$  cluster is consistent with the fact that it is the most abundant cluster in the mass spectrum of  $\text{Au}_n\text{Zn}^+$  ( $n=2-44$ ). Other high-symmetry clusters discussed in this Review, such as  $\text{B}_9^-$  or  $\text{Ta@B}_{10}^-$ , also meet these requirements due to the presence of  $\sigma$ -delocalized elements, while being the most favorable isomers out of a myriad of other possible structures and multiplicities based on the calculations and experimental photoelectron spectra analyses. As for the solid-state compounds, we believe that they can indeed be claimed  $\sigma$ -aromatic if they feature delocalized  $\sigma$ -bonding, highly symmetric geometries, and they are experimentally accessible. Certainly, many magnetic criteria can also be helpful to further assess the presence of  $\sigma$ -aromaticity in novel clusters and molecules, but some precautions must be taken into account.<sup>[74,75]</sup>

Overall, we believe that as long as  $\pi$ -aromaticity and  $\pi$ -antiaromaticity concepts are a part of the chemical lexicon, we should accept the  $\sigma$ -aromaticity and  $\sigma$ -antiaromaticity concepts as well. If we accept only  $\sigma$ -delocalized bonding but not  $\sigma$ -aromaticity or  $\sigma$ -antiaromaticity, we will create two parallel languages in chemistry. Hence, there is no reason to believe that  $\sigma$ -aromaticity and  $\sigma$ -antiaromaticity will not be a part of chemistry any time soon. In this Review we demonstrated that  $\sigma$ -aromatic and  $\sigma$ -antiaromatic chemical species have the same pattern of delocalized bonds and exhibit similar geometrical structures as species featuring  $\pi$ -aromaticity/antiaromaticity. We showed that the  $\sigma$ -aromatic species are the most stable isomers among other alternative ones similar to the  $\pi$ -aromatic species. All that justifies the place of  $\sigma$ -aromaticity and  $\sigma$ -antiaromaticity in chemistry. So, why deny the same treatment of  $\sigma$ - and  $\pi$ -bonding concepts?

We hope that in this Review we have demonstrated that  $\sigma$ -aromaticity and  $\sigma$ -antiaromaticity are useful tools in deciphering chemical bonding in clusters, molecules, and solid-state compounds. We believe that these concepts will also be helpful beyond organic and inorganic chemistries in areas such as material science, catalysis, nanotechnology, biochemistry, and many other fields of science.

## Acknowledgements

The authors thank the Ministry of Education and Science of the Russian Federation (megagrant of the Russian Government to support scientific research under the supervision of the leading scientist at Southern Federal University, no. 14.Y26.31.0016) and A.I.B. thanks the National Science Foundation of the U.S. (grant CHE-1361413) for financial support.

## Conflict of interest

The authors declare no conflict of interest.

**Keywords:** AdNDP · bond theory · multiple antiaromaticity · multiple aromaticity ·  $\sigma$ -antiaromaticity ·  $\sigma$ -aromaticity

- [1] A. Kekulé, *Bull. Soc. Chim. Fr.* **1865**, 3, 98–110.  
 [2] A. Kekulé, *Bull. Acad. R. Belg.* **1865**, 119, 551–563.  
 [3] A. Kekulé, *Ann. Chem. Pharm.* **1865**, 137, 129–196.  
 [4] E. Z. Hückel, *Z. Phys.* **1931**, 70, 204–286.  
 [5] E. Z. Hückel, *Z. Phys.* **1932**, 76, 628–648.  
 [6] R. Breslow, *Chem. Eng. News* **1965**, 43, 90–100.  
 [7] R. Breslow, *Acc. Chem. Res.* **1973**, 6, 393–398.  
 [8] A. I. Boldyrev, L. S. Wang, *Chem. Rev.* **2005**, 105, 3716–3757.  
 [9] C. A. Tsipis, *Coord. Chem. Rev.* **2005**, 249, 2740–2762.  
 [10] A. N. Alexandrova, A. I. Boldyrev, H. J. Zhai, L. S. Wang, *Coord. Chem. Rev.* **2006**, 250, 2811–2866.  
 [11] D. Yu. Zubarev, B. B. Averkiev, H.-J. Zhai, L. S. Wang, A. I. Boldyrev, *Phys. Chem. Chem. Phys.* **2008**, 10, 257–267.  
 [12] D. Yu. Zubarev, A. I. Boldyrev in *Computational Inorganic and Bioinorganic Chemistry* (Ed.: E. I. Solomon, R. A. Scott, R. B. King), Wiley, Chichester, **2009**, pp. 551–562.  
 [13] A. P. Sergeeva, B. B. Averkiev, A. I. Boldyrev in *Structure and Bonding: Metal-Metal Bonding* (Ed.: G. Parkin), Springer, Berlin, **2010**, 136, pp. 275–306.  
 [14] C. A. Tsipis in *Structure and Bonding: Metal-Metal Bonding* (Ed.: G. Parkin), Springer, Berlin, **2010**, 136, pp. 217–274.  
 [15] A. P. Sergeeva, A. I. Boldyrev in *Aromaticity and Metal Clusters* (Ed.: P. K. Chattaraj), CRC Press, Boca Raton, **2010**, pp. 55–68.  
 [16] T. R. Galeev, A. I. Boldyrev, *Annu. Rep. Prog. Chem. Sect. C* **2011**, 107, 124–147.  
 [17] F. Feixas, E. Matito, J. Poater, M. Solà, *Wiley Interdiscip. Rev.: Comput. Mol. Sci.* **2013**, 3, 105–122.  
 [18] I. A. Popov, A. I. Boldyrev in *The Chemical Bond: Chemical Bonding Across the Periodic Table* (Ed.: G. Frenking, S. Shaik), Wiley-VCH, Weinheim, **2014**, pp. 421–444.  
 [19] I. Fernández, G. Frenking, G. Merino, *Chem. Soc. Rev.* **2015**, 44, 6452–6463.  
 [20] J. M. Mercero, A. I. Boldyrev, G. Merino, J. M. Ugalde, *Chem. Soc. Rev.* **2015**, 44, 6519–6534.  
 [21] A. I. Boldyrev, L. S. Wang, *Phys. Chem. Chem. Phys.* **2016**, 18, 11589–11605.  
 [22] R. Hoffmann, *Am. Sci.* **2015**, 103, 18–22.  
 [23] S. Ritter, *Chem. Eng. News* **2015**, 93, 37–38.  
 [24] M. J. S. Dewar, *Bull. Soc. Chim. Belg.* **1979**, 88, 957–967.  
 [25] M. J. S. Dewar, M. L. McKee, *Pure Appl. Chem.* **1980**, 52, 1431–1441.  
 [26] W. Wu, B. Ma, J. I-Chia Wu, P. v. R. Schleyer, Y. Mo, *Chem. Eur. J.* **2009**, 15, 9730–9736.  
 [27] J. P. Foster, F. Weinhold, *J. Am. Chem. Soc.* **1980**, 102, 7211–7218.  
 [28] D. Y. Zubarev, A. I. Boldyrev, *Phys. Chem. Chem. Phys.* **2008**, 10, 5207–5217.  
 [29] A. P. Sergeeva, A. I. Boldyrev, *Comm. Inorg. Chem.* **2010**, 31, 2–12.  
 [30] B. D. Dunnington, J. R. Schmidt, *J. Chem. Theory Comput.* **2012**, 8, 1902–1911.  
 [31] T. R. Galeev, B. D. Dunnington, J. R. Schmidt, A. I. Boldyrev, *Phys. Chem. Chem. Phys.* **2013**, 15, 5022–5029.  
 [32] A. N. Alexandrova, A. I. Boldyrev, *J. Phys. Chem. A* **2003**, 107, 554–560.  
 [33] R. W. A. Havenith, F. De Proft, P. W. Fowler, P. Geerlings, *Chem. Phys. Lett.* **2005**, 407, 391–396.  
 [34] S. K. Ritter, *Chem. Eng. News* **2016**, 94, 28–29.  
 [35] L. Yong, S. D. Wu, X. X. Chi, *Int. J. Quantum Chem.* **2007**, 107, 722–728.  
 [36] P. v. R. Schleyer, C. Maerker, A. Dransfeld, H. Jiao, N. J. R. v. Eikema Hommes, *J. Am. Chem. Soc.* **1996**, 118, 6317–6318.  
 [37] H. Tanaka, S. Neukemans, E. Janssens, R. E. Silverans, P. Lievens, *J. Am. Chem. Soc.* **2003**, 125, 2862–2863.  
 [38] K. J. Taylor, C. Jin, J. Conceicao, L. S. Wang, O. Cheshnovsky, B. R. Johnson, P. J. Nordlander, R. E. Smalley, *J. Chem. Phys.* **1990**, 93, 7515–7518.  
 [39] H. Häkkinen, B. Yoon, U. Landman, X. Li, H. J. Zhai, L. S. Wang, *J. Phys. Chem. A* **2003**, 107, 6168–6175.  
 [40] T. Holtz, E. Janssens, N. Veldeman, T. Veszprem, P. Lievens, M. T. Nguyen, *ChemPhysChem* **2008**, 9, 833–838.  
 [41] T. Holtz, N. Veldeman, T. Veszpremi, P. Lievens, M. T. Nguyen, *Chem. Phys. Lett.* **2009**, 469, 304–307.  
 [42] L. Lin, P. Lievens, M. T. Nguen, *J. Mol. Struct.* **2010**, 943, 23–31.  
 [43] L. Lin, T. Holtz, P. Gruene, P. Claes, G. Meijer, A. Felicke, P. Lievens, M. T. Nguen, *ChemPhysChem* **2008**, 9, 2471–2474.  
 [44] X. Huang, H. J. Zhai, B. Kiran, L. S. Wang, *Angew. Chem. Int. Ed.* **2005**, 44, 7251–7254; *Angew. Chem.* **2005**, 117, 7417–7420.  
 [45] Q. Xu, L. Jiang, N. Tsumori, *Angew. Chem. Int. Ed.* **2005**, 44, 4338–4342; *Angew. Chem.* **2005**, 117, 4412–4416.  
 [46] C. Foroutan-Nejad, S. Shahbazian, P. Rashidi-Ranjbar, *Phys. Chem. Chem. Phys.* **2011**, 13, 4576–4582.  
 [47] T. J. Robilotto, J. Bacsá, T. B. Gray, J. P. Sadighi, *Angew. Chem. Int. Ed.* **2012**, 51, 12077–12080; *Angew. Chem.* **2012**, 124, 12243–12246.  
 [48] S. Blanchard, L. Fensterbank, G. Gontard, E. Lacote, G. Maestri, M. Malacria, *Angew. Chem. Int. Ed.* **2014**, 53, 1987–1991; *Angew. Chem.* **2014**, 126, 2018–2022.  
 [49] F. Fu, J. Xiang, H. Cheng, L. Cheng, H. Chong, S. Wang, P. Li, S. Wei, M. Zhu, Y. Li, *ACS Catal.* **2017**, 7, 1860–1867.  
 [50] A. Monfredini, V. Santacroce, P.-A. Deyris, R. Maggi, F. Bigi, G. Maestri, M. Malacria, *Dalton Trans.* **2016**, 45, 15786–15790.  
 [51] T. Kuwabara, H. D. Guo, S. Nagase, M. Saito, *Angew. Chem. Int. Ed.* **2014**, 53, 434–438; *Angew. Chem.* **2014**, 126, 444–448.  
 [52] I. A. Popov, F.-X. Pan, X.-R. You, L.-J. Li, E. Matito, C. Liu, H.-J. Zhai, Z.-M. Sun, A. I. Boldyrev, *Angew. Chem. Int. Ed.* **2016**, 55, 15344–15346; *Angew. Chem.* **2016**, 128, 15570–15572.  
 [53] J. Chandrasekhar, E. D. Jemmis, P. v. R. Schleyer, *Tetrahedron Lett.* **1979**, 20, 3707–3710.  
 [54] X. Li, A. E. Kuznetsov, H.-F. Zhang, A. I. Boldyrev, L. S. Wang, *Science* **2001**, 291, 859–861.  
 [55] A. E. Kuznetsov, A. I. Boldyrev, X. Li, L. S. Wang, *J. Am. Chem. Soc.* **2001**, 123, 8825–8831.  
 [56] H. J. Zhai, A. N. Alexandrova, K. A. Birch, A. I. Boldyrev, L. S. Wang, *Angew. Chem. Int. Ed.* **2003**, 42, 6004–6008; *Angew. Chem.* **2003**, 115, 6186–6190.  
 [57] T. R. Galeev, C. Romanescu, W. L. Li, L. S. Wang, A. I. Boldyrev, *Angew. Chem. Int. Ed.* **2012**, 51, 2101–2105; *Angew. Chem.* **2012**, 124, 2143–2147.  
 [58] A. N. Alexandrova, A. I. Boldyrev, H.-J. Zhai, L. S. Wang, E. Steiner, P. W. Fowler, *J. Phys. Chem. A* **2003**, 107, 1359–1369.  
 [59] A. N. Alexandrova, A. I. Boldyrev, H. J. Zhai, L. S. Wang, *J. Chem. Phys.* **2005**, 122, 054313.  
 [60] H.-J. Zhai, A. E. Kuznetsov, A. I. Boldyrev, L. S. Wang, *ChemPhysChem* **2004**, 5, 1885–1891.  
 [61] H. J. Zhai, L. S. Wang, A. N. Alexandrova, A. I. Boldyrev, *J. Chem. Phys.* **2002**, 117, 7917–7924.  
 [62] A. E. Kuznetsov, K. A. Birch, A. I. Boldyrev, X. Li, H. J. Zhai, L. S. Wang, *Science* **2003**, 300, 622–625.  
 [63] S. Ritter, *Chem. Eng. News* **2003**, 81, 8.  
 [64] B. B. Averkiev, A. I. Boldyrev, *J. Phys. Chem. A* **2007**, 111, 12864–12866.  
 [65] A. E. Kuznetsov, J. D. Corbett, L. S. Wang, A. I. Boldyrev, *Angew. Chem. Int. Ed.* **2001**, 40, 3369–3372; *Angew. Chem.* **2001**, 113, 3473–3476.  
 [66] H. J. Deiseroth, *Prog. Solid State Chem.* **1997**, 25, 73–123.  
 [67] J. W. Nielsen, N. C. Baenziger, *Acta Crystallogr.* **1954**, 7, 277–282.  
 [68] M. D. Wodrich, C. S. Wannere, Y. Mo, P. D. Jarowski, K. N. Houk, P. v. R. Schleyer, *Chem. Eur. J.* **2007**, 13, 7731–7744.  
 [69] C. R. Kemnitz, J. L. Mackey, M. L. Loewen, J. L. Hargrove, J. L. Lewis, W. E. Hawkins, A. F. Nielsen, *Chem. Eur. J.* **2010**, 16, 6942–6949.  
 [70] Y. Mo, P. C. Hiberty, P. v. R. Schleyer, *Theor. Chim. Acta* **2010**, 127, 27–38.  
 [71] T. C. Dinadayalane, U. D. Priyakumar, G. N. Sastry, *J. Phys. Chem. A* **2004**, 108, 11433–11448.  
 [72] I. Gagliardi, S. Evagelisti, V. Barone, B. O. Roos, *Chem. Phys. Lett.* **2000**, 320, 518–522.  
 [73] M. Tobita, R. J. Bartlett, *J. Phys. Chem. A* **2001**, 105, 4107–4113.  
 [74] L. Zhao, R. Grande-Aztatzi, C. Foroutan-Nejad, J. M. Ugalde, G. Frenking, *ChemistrySelect* **2017**, 2, 863–870.  
 [75] F. Feixas, E. Matito, M. Duran, J. Poater, M. Solà, *Theor. Chem. Acc.* **2011**, 128, 419–431.

Manuscript received: May 8, 2017

Accepted manuscript online: June 7, 2017

Version of record online: October 17, 2017